Spatially separated excitons in quantum-dot quantum well structures

Kai Chang and Jian-Bai Xia
National Laboratory for Superlattices and Microstructures, Institute of Semiconductors, Chinese Academy of Sciences, P.O. Box 912, Beijing 100083, People's Republic of China
(Received 15 August 1997)

In the framework of the effective-mass envelope-function theory, the electronic and optical properties of a spherical core-shell quantum-dot quantum well (QDQW) structure with one and two wells have been investigated. The results show that the energies of electron and hole states depend sensitively on the well thickness and core radius of quantum-dot quantum well structure. An interesting spatially separated characteristic of electron and hole in QDQW is found and enhanced significantly in the two-wells case. The normalized oscillator strength for the optical transition between the electron and hole states in QDQW exhibits a deep valley at some special well thickness. The Coulomb interaction between the electron and hole is also taken into account. [S0163-1829(98)02412-6]

I. INTRODUCTION

At present, much attention is paid to the physics of low-dimensional semiconductor structures. This has been stimulated by the rapid progress in nanometer-scale fabrication technology. Among those, quantum dots (QD's) are of particular interest.[1] The effect of quantum confinement on the electrons and holes in semiconductor QD has been studied extensively in recent years.[2–5] The most striking properties of semiconductor quantum dots is the massive change in optical properties as a function of quantum-dot size. For example, the band gap in CdS can be tuned between 4.5 and 2.5 eV as the size is varied from the molecular regime to the macroscopic crystal.

It is possible now to fabricate various semiconductor quantum dots consisting of II-VI, III-V, and group IV semiconductor materials. Recently, a remarkable nanocrystal heterostructure called quantum-dot quantum well (QDQW) structure was synthesized, which is composed of two different semiconductor materials[6] (shown as Fig. 1). It consists of a tetrahedral CdS core, about 50 Å in size, with (111) facets. When exposed to Hg^{2+} ions, the Hg^{2+} displaces precisely 1 ML of Cd^{2+} from the surface. Subsequently, the HgS layer may be capped with a final layer of CdS. The resulting sample can be described as a CdS/HgS/CdS QDQW. The wet chemical synthesis, the characterization, and some linear and nonlinear optical properties of QDQW have recently been reported in detail.[6–8] It has been shown that the linear absorption of QDQW differs significantly from that of the composite materials. The transition energy (or new band gap) can be tuned by the core diameter, the thickness of the well, and the thickness of the outmost shell. The synthesis goals of the new type of quantum dot are the preparation of multiply layered structures giving multiple-quantum-dot quantum well, and the use of materials other than CdS and HgS. It is important to know the physical properties of these complex multilayer structures.

Haus *et al.*[9] developed a recursive method to calculate the electronic structure of QDQW. They assumed the infinite potential well and calculated $1s$-$1s$ transition energies, neglecting the Coulomb interaction between electron and hole. They found a tendency for the wave function amplitude to increase in the center, when a shell material of a smaller band gap is added to the core, while keeping the radius constant. Schooss *et al.*[10] considered a more realistic case, in which the effects of finite band offset and the Coulomb interaction between electron and hole were taken into account. They calculated the electronic structure of QDQW and compared with the experimental measurement.

The previous work is extended in two ways: first, higher excited states are investigated and they exhibit much different characteristics from the ground state, and second, we study the electronic structure of QDQW with two-well struc-

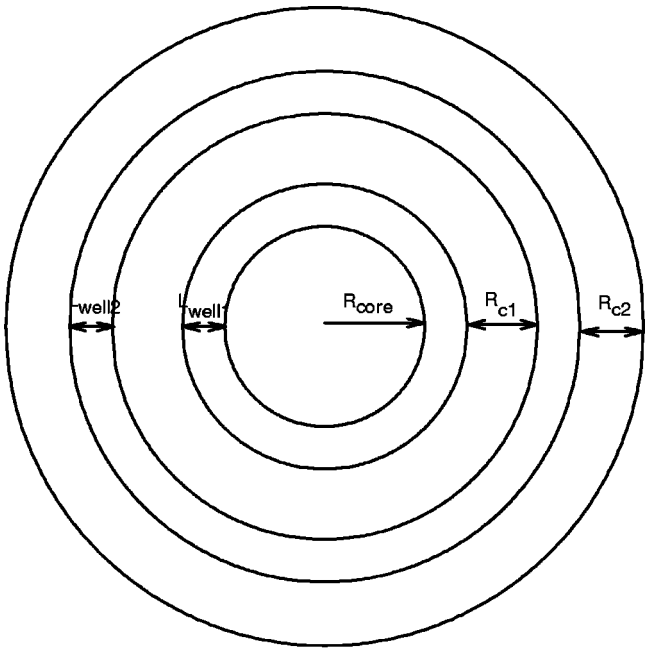

FIG. 1. The schematic structure of the quantum-dot quantum well.

ture. In this structure, with the electronic structure of QDQW significantly distinct from that of QD, it exhibits anticrossing between levels with the same angular momentum and crossing between levels with different angular momentum, and enhances the spatial separation characteristic of the exciton in QDQW. We found that the binding energy is suppressed but the pair-oscillator strength is enhanced by adding an addtional well to a quantum dot. It provides a flexibility to tailor the wave functions of electron and hole in QD. The mechanism of spatially separated character is different from that caused by the external electric field, which results in weakening of the oscillator strength and widening of the linewidth. One possible application is as follows: the spatially separated character results in a long lifetime exciton and large dipole moment, and consequently enhances its nonlinear optical properties in weak field. It may provide a basis for a new type of opticelectronic device. We will deal with the problem in a forthcoming paper.

In this paper we shall propose a numerical diagonalization method to calculate the electronic structures of semiconductor quantum-dot quantum well structure. Our method is convenient to apply to these complex multilayered structures and agree well with experiment measurement. The excitonic energies including the Coulomb interaction are calculated. For simplicity, we use the simple-parabolic-band model for electron and hole, neglecting the mixing effect of heavy and light hole states. The mixing effect can be taken into account conveniently in our method. The paper is organized as follows: Sec. II presents the calculation method and deals with optical transition probabilities. Section III gives the numerical results on electronic structure of the quantum-dot quantum well. Finally, we give the conclusion in Sec. IV.

II. CALCULATION METHOD

We consider a spherical QDQW consisting of several layers, one semiconductor material with a smaller band gap sandwiched by another material with a larger band gap; the whole QDQW is embedded in water matrix. The eigenstates of the exciton in QDQW structures can be expanded in terms of the uncorrelated pair states constructed from single particle states for electron and hole in the QDQW. The eigenstates of electron and hole are obtained from the numerical diagonalized method. We assumed the spherical QDQW embedded in a big sphere with radius $R_{\max}$. The complete basis set is constructed from the spherical Bessel function. Our method is convenient to apply to those complex structure with multilayers and external field.

If we take the electronic Bohr radius and Rydberg $a_e^* = \hbar^2 \epsilon_0 / m_0 e^2$ as units of length and energy, the exciton Hamiltonian in a QDQW structure can be written as

$$H = H_0 + V_{e\text{-}h}, \tag{1}$$

$$H_0 = \mathbf{P}_e \frac{1}{m_e^*(r)} \mathbf{P}_e + \mathbf{P}_h \frac{1}{m_h^*(r)} \mathbf{P}_h + V_e(r) + V_h(r), \tag{2}$$

$$V_{e\text{-}h} = -\frac{2}{\epsilon(r_e, r_h) r_{eh}}, \tag{3}$$

where e (h) refers to electron (hole), $\epsilon(r_e, r_h)$ the dielectric constant of the materials, m_e (m_h) the effective mass of electron (hole) in units of the free electron mass m_0. $V_{e\text{-}h}$ is the Coulomb interaction term between the electron and hole, $V_e(V_h)$ the confined potential of electron and hole in the QDQW,

$$V_i(\mathbf{r}) = \begin{cases} V_{i1}, & r < R_1 \\ 0, & R_1 < r < R_2 \\ V_{i2}, & R_2 < r < R_3 \\ 0, & R_3 < r < R_4 \\ V_{i3}, & R_4 < r < R_5 \\ \vdots & \vdots \\ V_{in}, & R_{n-1} < r < R_n \\ \vdots & \vdots \end{cases} \tag{4}$$

$$m_i^*(\mathbf{r}) = \begin{cases} m_{i1}^*, & r < R_1 \\ m_{b1}^*, & R_1 < r < R_2 \\ m_{i2}^*, & R_2 < r < R_3 \\ m_{b2}^*, & R_3 < r < R_4 \\ m_{i3}^*, & R_4 < r < R_5 \\ \vdots & \vdots \\ m_{in}^*, & R_{n-1} < r < R_n \\ \vdots & \vdots \end{cases} \tag{5}$$

where the subscript $i = e, h$ denotes the electron or hole.

The exciton wave function can be expanded in terms of single-particle wave function

$$\Psi_{ex} = \sum_{i,j} c_{ij} \Psi_{ei}(r_e) \Psi_{hj}(r_h) \tag{6}$$

where $\Psi_{ei}(r_{ei})$ and $\Psi_{hj}(r_{hj})$ are the wave functions of electronic and hole eigenstates, respectively. The matrix element of the Coulomb interaction can be calculated by using

$$\frac{1}{\epsilon(r_e, r_h) r_{eh}} = \sum_{k=0}^{\infty} \frac{r_<^k}{\epsilon(r_e, r_h) r_>^{k+1}} P_k(\cos\theta_{eh}), \tag{7}$$

$$P_k(\cos\theta_{eh}) = \frac{4\pi}{2k+1} \sum_{m=-k}^{k} Y_{km}^*(\theta_e, \varphi_e) Y_{km}(\theta_h, \varphi_h), \tag{8}$$

where P_k are the Legendre polynomials, θ_{eh} is the angle between the position vector of electron (r_e) and hole (r_h), $r_< \equiv \min(r_e, r_h)$ and $r_> \equiv \max(r_e, r_h)$.

The exciton energy can be obtained from secular equation

$$\left| (E_{n_e, l_e} + E_{m_h, l_h} - E) \delta_{ij} + V_{ij} \right| = 0 \tag{9}$$

the matrix element of the Coulomb interaction V_{ij} is given by

$$\left\langle \frac{1}{r_{eh}} \right\rangle = \sum_k R^k \frac{4\pi}{2k+1} \sum_{m=-k}^{k} (-1)^m \langle Y_{l_e' m_e'} | Y_{k-m} | Y_{l_e m_e} \rangle \langle Y_{l_h' m_h'} | Y_{km} | Y_{l_h m_h} \rangle \tag{10}$$

where

$$R^k = \int_0^\infty \int_0^\infty R_e(n_e, l_e, m_e) R_e(n_e', l_e', m_e') R_h(n_h, l_h, m_h) R_e(n_h', l_h', m_h') \frac{r_<^k}{r_>^{k+1}} r_e^2 r_h^2 dr_e dr_h, \tag{11}$$

$$\langle Y_{l'm'} | Y_{km} | Y_{lm} \rangle = \int_0^{2\pi} \int_0^{\pi} Y_{l'm'}(\theta,\varphi) Y_{km}(\theta,\varphi) Y_{lm}(\theta,\varphi) \sin(\theta) d\theta d\varphi$$

$$= \left[\frac{(2l'+1)(2l+1)(2k+1)}{4\pi} \right]^{1/2} \begin{pmatrix} k & l_h & l_h' \\ 0 & 0 & 0 \end{pmatrix} \begin{pmatrix} k & l_h & l_h' \\ m & m_h & m_h' \end{pmatrix}. \tag{12}$$

The Hamiltonian of the electron is

$$H_e = \mathbf{P}_e \frac{1}{m_e^*(\mathbf{r})} \mathbf{P}_e + V_e(\mathbf{r}),$$
$$H_e \Psi_e(\mathbf{r}) = E_n \Psi(\mathbf{r}). \tag{13}$$

$\Psi(r_e)$ satisfies the boundary condition

$$\Psi_e(R_{\max}, \theta, \varphi) = 0, \tag{14}$$

where $R_{\max}$ is the radius of the large sphere. The spherical Bessel function in large sphere constitute a complete orthonormal basis of single-particle wave function.

The angular quantum number l and its z component m are both good quantum numbers, the wave function of the electron respect to l and m can be written as

$$\Psi(r_e, \theta, \varphi) = \sum_n a_{nl} A_{nl} j_l(k_n^l r_e) Y_{lm}(\theta, \varphi). \tag{15}$$

$A_{nl} = (\sqrt{2}/R^{3/2}) 1/j_l(\alpha_n^l)$ is the normalization constant, j_l the spherical Bessel function of lth order. $\alpha_n^l = k_n^l R_{\max}$ is the nth zero points of j_l. $R_{\max}$ is determined by convergence of the energy of electron in QDQW. Here we take $R_{\max} = 2R_{\mathrm{QDQW}}$ in the calculation.

By substituting Eq. (15) into Eq. (13), we obtained easily a $n \times n$ secular equation for the coefficients a_n:

$$|H_{ij} - E\delta_{ij}| = 0, \tag{16}$$

where $H_{ij} = \int f(r_e)_j \hat{H}_e f(r_e)_i r_e^2 dr_e$. Solving the secular equation by the matrix diagonalization method, we obtain eigenenergies and corresponding eigenstates not only for the ground states but also excited states.

The eigenstates of the hole in QDQW can be obtained by similar procedure. The valence-band mixing effect has been investigated in detail.[11–14] Since the mixing effect is weak for size of QDQW concerned here (2–10 nm), we neglect the valence band mixing effect here for simplicity. The cluster band-structure calculation supports this conclusion over the size range in our calculation.[15–18] We assume that the electron and hole are confined in a spherical QDQW. The QDQW is embedded in a large sphere with radius $R_{\max}$. Since we are only concerned with the localized states in QDQW, the numerical results will converge if the radius $R_{\max}$ and the number of basis states involved in calculation are large enough.

The optical transition probability between the electron and hole states can be calculated by[19]

$$\langle \Phi_e | \mathbf{p} | \Phi_h \rangle = \int r^2 dr f_e(r) f_h(r) \langle l_e m_e | l_h m_h \rangle \langle c | \mathbf{p} | v \rangle \tag{17}$$

$$= \sum_L \int r^2 dr f_e(r) f_h(r) \sum_{M_1} \langle c | \mathbf{p} | v \rangle \tag{18}$$

$$= I_{eh} \mathbf{p}_{cv} \delta_{l_e l_h} \delta_{m_e m_h}, \tag{19}$$

TABLE I. Material parameters. All energies are in units of eV, m_e^* is effective mass of the electron in units of the free-electron mass; E_g is the band gap, V_{c1} the conduction band offset.

Material	m_e^*	m_h^*	E_g	V_{c1}	ϵ_∞
CdS	0.2	0.7	2.5	1.35	5.5
HgS	0.036	0.44	0.5		11.36
CdSe	0.13	0.45	1.84		9.8
ZnS	0.28	0.49	3.9	0.9	
H_2O	1	1	3.		1.78

TABLE II. Calculated energies of the transition eneries between $1S_e$-$1S_h$ for HgS/CdS QDQW. Experimental transition energies are also given (Ref. 10) (in units of eV).

R_{core} (nm)	2.35	2.35	2.35
L_{well} (nm)	0.3	0.6	0.9
R_{clad} (nm)	0.3	0.3	0.3
$1s_e$-$1S_{3/2}$	2.31	1.9	1.72
Expt.	2.1	1.76	1.6

where $|c\rangle$ and $|v\rangle$ are the Bloch wave functions at the conduction-band bottom and valence-band top. I_{eh} is the overlap integral.

III. NUMERICAL RESULTS AND DISCUSSION

The structure of a spherical QDQW embedded in water matrix involved in calculation is shown schematically in Fig. 1. The material parameters used in the calculation are listed in Table I. We investigate the energies of the electron and hole states for CdS/HgS and ZnS/CdSe QDQW structures. An interesting spatially separated characteristic of excitons in QDQW structure is found and enhanced significantly for two wells case. The comparison between theoretical results and experimental measurement for HgS/CdS is listed in Table II.

In a QDQW structure, we studied the energies of electron levels with angular momentum $l=0,1,2$ for various well thickness. The energies of the lowest two electron energy levels for ZnS/CdSe and HgS/CdS QDQW's with one well and two wells are showed in Fig. 2 [(a), (b), (c), and (d)] as a function of the well thickness, respectively. The dependence of energies of electron and hole level on the well thickness is comparatively more complicated in QDQW structure. In the QD case, the energies decrease approximately quadratically with radius of QD and no crossing between levels with different angular momentum (or anticrossing between same angular momentum) occurs. In the QDQW with one well case [Figs. 2(a) and 2(b)], the wave function of the lowest level of electron localized in the well region and its energies depend sensitively on the well thickness rather than the core radius. The energies of second level are insensitive to the well thickness, since its energies are higher than the conduction band bottom of barrier material (ZnS or CdS) and its wave function extends to the whole region of QDQW. When the well thickness increases continuously, the wave function of the second level localized in the well region and its energies decrease rapidly. The energy spectra of ZnS/CdSe and HgS/CdS QDQW's with two wells are shown in Figs. 2(c) and 2(d) as a function of the outer well thickness, respectively. The crossing between levels with different

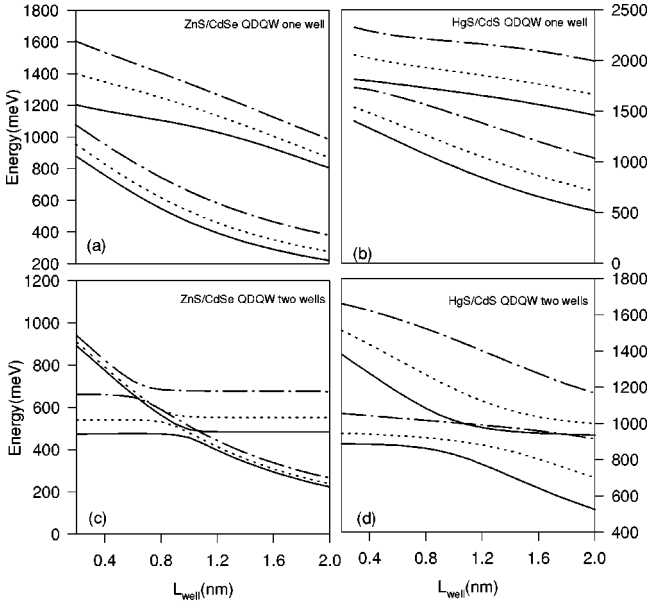

FIG. 2. The energies of the electron states of angular momentum l=0 (solid line), 1 (dotted line), 2 (dashed line) in ZnS/CdSe QDQW vs the well thickness. (a) [(b)] plots the electron in ZnS/CdSe (HgS/CdS) QDQW with one well, $R_{\text{core}}=2.35$ nm, $R_{c1}=1$ nm and (c) [(d)] plots the electron in ZnS/CdSe (HgS/CdS) QDQW with two wells case. $R_{\text{core}}=2.35$ nm, $L_{\text{well1}}=1$ nm, $R_{c1}=2$ nm, $R_{c2}=1$ nm.

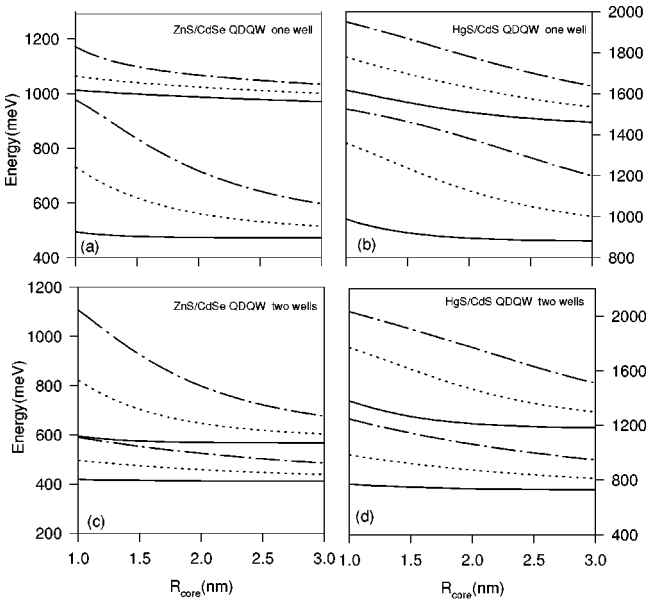

FIG. 3. The energies of the electron states of angular momentum $l=0$ (solid line), 1 (dotted line), 2 (dashed line) in ZnS/CdSe QDQW vs the radius of core. (a) [(b)] plots the electron in ZnS/CdSe (CdS/HgS) QDQW with one well, $L_{\text{well1}}=1$ nm, $R_{c1}=3$ nm and (c) [(d)] plots the electron (hole) in QDQW with two wells case. $L_{\text{well1}}=1$ nm, $L_{\text{well2}}=1$ nm, $R_{c1}=1$ nm, $R_{c2}=1$ nm.

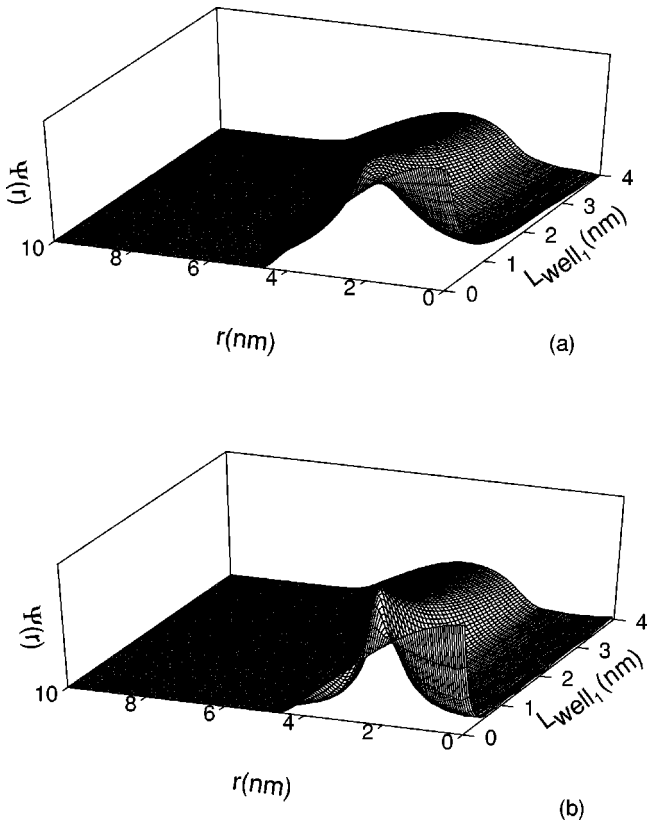

FIG. 4. The wave function of the (a) electron and (b) hole states of angular momentum $l=0$ in ZnS/CdSe QDQW with one well vs the well thickness and radius of core.

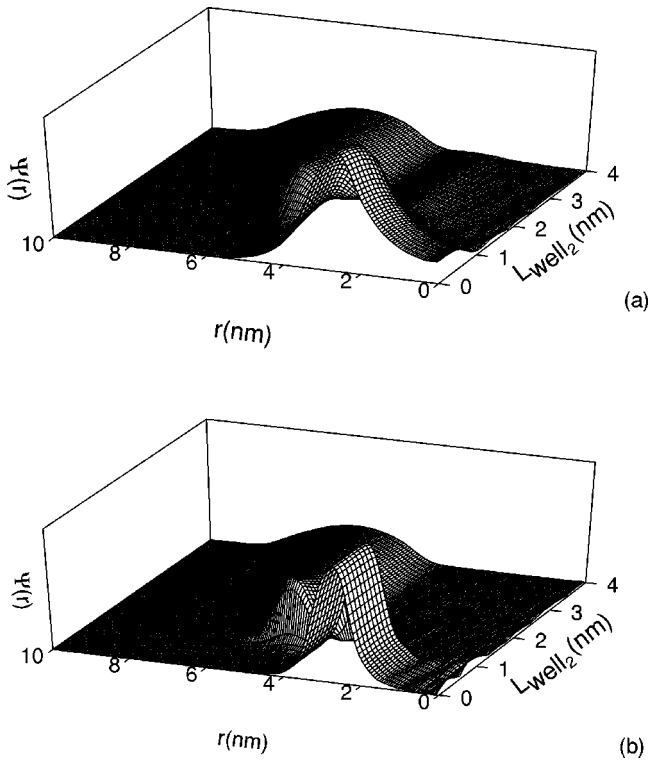

FIG. 5. The wave function of the (a) electron and (b) hole states of angular momentum $l=0$ in ZnS/CdSe QDQW with two wells vs the outer well thickness and radius of core.

angular momentum and anticrossing between levels with the same angular momentum can be observed in these figures. The wave functions of the lowest energy level are always localized in the internal well, while the wave functions of the second level localized in the outer well region of QDQW though the outer well is narrow to 0.4 nm (the thickness of the internal well thickness L_{well} is 1 nm), thus the energies of the lowest level are almost constant, and the energies of the second level decrease rapidly when the outer well becomes wider. When the energies of two states in two wells are close to each other, then the anticrossing and crossing occurs as seen from Figs. 2(c) and 2(d). Comparing Figs. 2(a) and 2(b) [(c) and (d)], we found that for smaller effective masses (CdS/HgS QDQW), the energy level of different angular momentum separates farther. The energy spectra of hole states in these two QDQW's are similar.

Figure 3 illustrates the energies of electron states of angular momentum $l=0,1,2$ varying with the radius of core of ZnS/CdSe and HgS/CdS QDQW with one well [Figs. 3(a) and 3(b)] and two wells [Figs. 3(c) and 3(d)], respectively. From these figures, we find that energies of electron states with $l=0$ are insensitive to the radius of core of QDQW, the energies of the states with $l=1,2$ decrease rapidly with increase of the core radius. This result arises from the fact that the electron at the $l=0$ level is trapped in the well region, but those at the $l=1,2$ level extend over the whole region of QDQW. When the core radius increases, the variations of confinement are slight for electron at the level of $l=0$, but large for those at the levels of $l=1,2$.

Figures 4(a) and 4(b) depict the wave functions of electron and hole ground states of $l=0$ in ZnS/CdSe QDQW with one well. The results show that the wave function of the electron and the hole concentrate in the center of the QD while the well is narrow, and shift toward a wider well region at a different rate while well thickness increases. Figures 5(a) and 5(b) show the wave function of electron and hole ground states of $l=0$ in ZnS/CdSe QDQW with two wells. The wave function of the electron and hole concentrate in the internal well initially; when the outer well thickness increases and the anticrossing occurs, the electron and hole move to the outer well. Due to the difference of the effective mass and confinement between electron and hole, the electron (hole) localizes at a different region for specific size of QDQW. This phenomenon can be observed readily in these figures when the outer well thickness approaches $L_{\text{well2}}=1$ nm for the structure involved in the calculation. An interesting spatially separated characteristic between electron and hole can be observed.

In Figs. 6(a) and 6(b) we plot the overlap integral I_{eh} between $1S_h$ and $1S_e$ as a function of the radius of core and thickness of well. In these figures we can find that spatial separation between electron and hole exists in the QDQW structures containing one [Fig. 6(a)] or two wells [Fig. 6(b)]. This arises from the difference between the effective masses and confinement of electron and hole. The spatial separation characteristic of the exciton cannot be observed in QD's without internal wells. The overlap integral decreases to a minimum, and then increases continuously with increasing well thickness. It is enhanced for QDQW in the two-wells case. The overlap integral in QDQW containing two wells

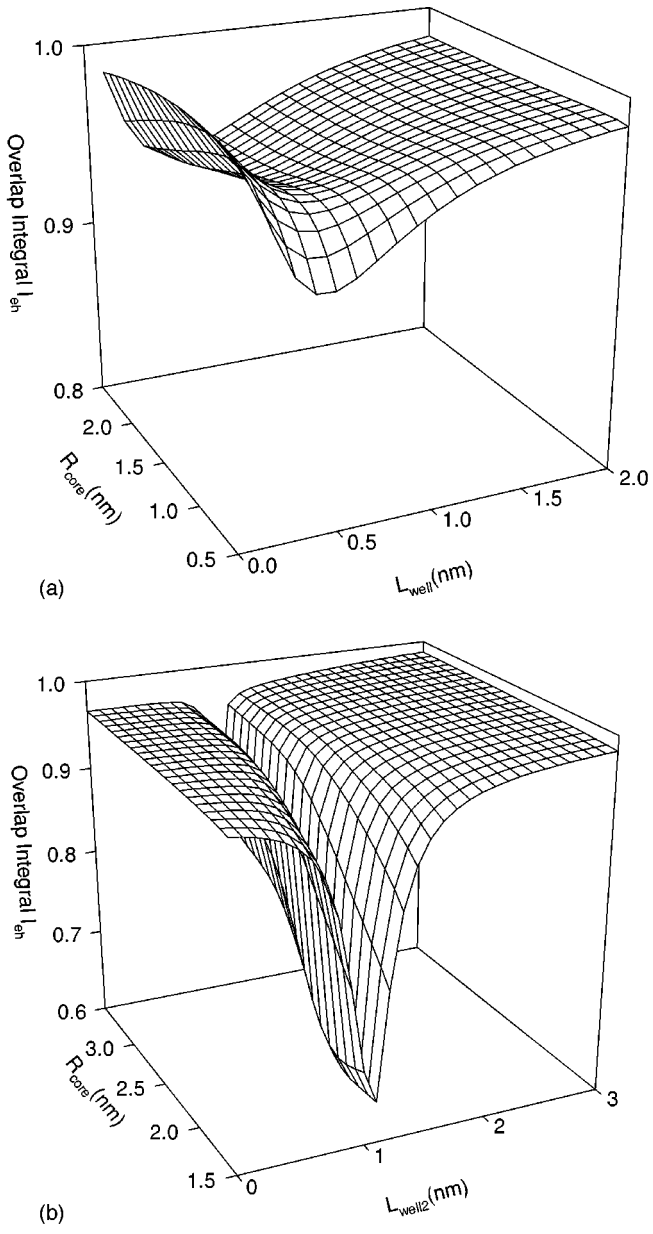

FIG. 6. The overlap integral I_{eh} between the electron and hole states of angular momentum $l=0$ in ZnS/CdSe QDQW with (a) one well and (b) two wells vs the well thickness and radius of core.

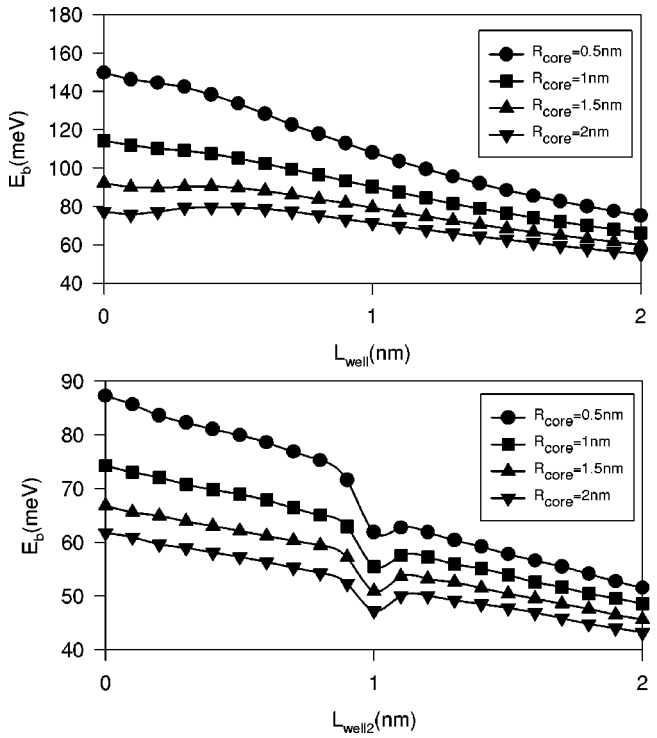

FIG. 7. The binding energy E_b of the ground state of exciton $(1S_e1S_h)$ in ZnS/CdSe QDQW with one well (a) $R_{c1}=1$ nm and two wells (b) vs the well thickness and radius of core. $L_{\text{well1}}=1$ nm, $R_{c1}=1$ nm, $R_{c2}=1$ nm.

exhibits a sharp valley in the range of specific size and a dramatic enhancement of spatial separation. The phenomenon can be explained as follows: while there is no internal well in the QD, the wave function of the electron and hole peak at the center of the QD. When the well thickness increases, the electron (hole) shifts to the well region at a different rate, and thus the overlap integral decreases to a minimum. QDQW containing two wells exhibits a strong spatial separation characteristic since electron and hole are trapped in different wells for special well thickness. The spatial separation characteristic can be enhanced or weakened by adjusting thickness of the clad layer between two wells.

Figure 7 shows how the binding energies of exciton of angular momentum $l=0$ varies with the well thickness for different core radius of QDQW. We find that the binding energy in QDQW is distinct from that in the QD case. The binding energy decreases monotonically in the QD case, but in QDQW structures with one well [Fig. 7(a)] the binding energies experience a minimum when the well thickness increases. The binding energies in the QDQW structure with two wells [Fig. 7(b)] exhibit a sharp valley when the well thickness increases. This phenomenon arises from the spatial separation between electron and hole. When the width of the outer well is small, electron and hole both localize in the first well. Electron and hole shift to the outer well at different rates with increasing outer well thickness, they are trapped in different well regions at some special size, thus the binding energy decreases. When the outer well thickness increases continuously, electron and hole are both trapped in the outer well and this leads to an increase of the binding energies. The competition between the spatial separation and the change of confinement of electron and hole results in these phenomena in the binding energy of the exciton.

IV. CONCLUSION

In this paper, we study the electronic structures of spherical QDQW structure with one and two wells, including the Coulomb interaction between electron and hole. It is found that the energies of the electron and hole depend sensitively on the structures of the QDQW, the crossing between the levels of electron and hole with different angular momentum, and anticrossing between the levels with same angular momentum can be observed in QDQW with two wells, and become remarkable in ZnS/CdSe QDQW structures. The spatial separation between electron and hole in QDQW with

two wells is more significant than that in QDQW with one well. The normalized oscillator strength for the optical transition between the electron and hole states in QDQW with two wells exhibits a deep valley at some special well thickness due to the difference of the electron and hole effective masses. Controlling size and composition of the materials of QDQW can provide the flexibility to engineer the electronic structure of QDQW and enhance or weaken spatial separation characteristic of the exciton in QDQW. The character will enhance the nonlinear optical properties of QD.

ACKNOWLEDGMENT

This work was supported by the Chinese National Natural Science Foundation.

[1] A. P. Alivisatos, Science **271**, 933 (1996), and references therein.
[2] A. I. Ekimov and A. A. Onushchenko, Pis'ma Zh. Éksp. Teor. Fiz. **34**, 363 (1981) [JETP Lett. **34**, 345 (1981)]; **40**, 337 (1984) [**40**, 1137 (1984)].
[3] Al. L. Efros and A. L. Efros, Sov. Phys. Semicond. **16**, 772 (1982).
[4] L. E. Brus, J. Chem. Phys. **80**, 4403 (1984).
[5] R. Rossetti, R. Hull, J. M. Gibson, and L. E. Brus, J. Chem. Phys. **82**, 552 (1985).
[6] A. Mews, A. Eychmüller, M. Giersig, D. Schooss, and H. Weller, J. Phys. Chem. **98**, 934 (1994).
[7] A. Eychmüller, A. Mews, and H. Weller, Chem. Phys. Lett. **208**, 59 (1993).
[8] A. Eychmüller, T. Vossmeyer, A. Mews, and H. Weller, J. Lumin. **58**, 223 (1994).
[9] J. W. Haus, H. S. Zhou, I. Honma, and H. Komiyama, Phys. Rev. B **47**, 1359 (1993).
[10] D. Schooss, A. Mews, A. Eychmüller, and H. Weller, Phys. Rev. B **49**, 17 072 (1994).
[11] J. B. Xia, Phys. Rev. B **40**, 8500 (1989).
[12] G. B. Grigorian, E. M. Kazaryan, Al. L. Efros, and T. V. Yazeva, Sov. Phys. Solid State **32**, 1031 (1990).
[13] P. C. Sercel and K. J. Vahala, Phys. Rev. B **42**, 3690 (1990).
[14] A. I. Ekimov, F. Hache, M. C. Schanne-Klein, D. Ricard, G. Flytzanis, I. A. Kudryavtsev, T. V. Yazeva, A. V. Rodina, and Al. L. Efros, J. Opt. Soc. Am. B **10**, 100 (1993).
[15] P. E. Lippens and M. Lannoo, Phys. Rev. B **39**, 10 935 (1989).
[16] M. V. RamaKrishna and R. A. Friesner, Phys. Rev. Lett. **67**, 629 (1991); S. V. Nair, L. M. Ramanish, and K. C. Rustagi, Phys. Rev. B **45**, 5969 (1992).
[17] Y. Wang and N. Herron, Phys. Rev. B **42**, 7253 (1990).
[18] G. T. Einevoll, Phys. Rev. B **45**, 3410 (1992).
[19] A. R. Edmonds, in *Angular Momentum in Quantum Mechanics* (Princeton University Press, Princeton, 1957).